Nonlinear Feedback Control of a Dual-Stage Actuator System for Reduced Settling Time

Jinchuan Zheng and Minyue Fu, *Fellow, IEEE*

Abstract—This brief presents a nonlinear control method for dual-stage actuator (DSA) systems to track a step command input fast and accurately. Conventional tracking controllers for DSA systems are generally designed to enable the primary actuator to approach the setpoint without overshoot. However, this strategy is unable to achieve the minimal settling time when the setpoints are beyond the secondary actuator travel limit. To further reduce the settling time, we design the primary actuator controller to yield a closed-loop system with a small damping ratio for a fast rise time and certain allowable overshoot. Then, a composite nonlinear control law is designed for the secondary actuator to reduce the overshoot caused by the primary actuator as the system output approaches the setpoint. The proposed control method is applied to an actual DSA positioning system, which consists of a linear motor and a piezo actuator. Experimental results demonstrate that our approach can further reduce the settling time significantly compared with the conventional control.

Index Terms—Dual-stage actuator, friction, linear motor, motion control, piezo actuator (PA), saturation.

I. INTRODUCTION

A DUAL-STAGE actuator (DSA) servo system is characterized by a structural design with two actuators connected in series along a common axis. The primary actuator (coarse actuator) is of long travel range but with poor accuracy and slow response time. The secondary actuator (fine actuator) is typically of higher precision and faster response but with a limited travel range. By combining the DSA system with properly designed servo controllers, the two actuators are complementary to each other and the defects of one actuator can be compensated by the merits of the other one. Therefore, the DSA system can provide large travel range, high positioning accuracy and fast response. The DSA servomechanism has been widely utilized in the industry, e.g., the dual-stage hard disk drive (HDD) actuator [1], [2]. The dual-stage HDD servomechanism can significantly increase the servo bandwidth to lower the sensitivity to various disturbances and thus push the track density [3]. Other DSA systems include the dual-stage machine tools [4], macro/micro robot manipulators [5], and dual-stage XY positioning tables [6], [7].

Although the mechanical design of a DSA system appears to be simple, it is a challenging task to design controllers for the two actuators to yield an optimal performance because of the specific characteristics in the DSA systems.

1) The DSA system is a dual-input single-output (DISO) system, which means that for a given desired trajectory,

alternative inputs to the two actuators are not unique. Thus, a proper control strategy is required for control allocation.

2) The secondary actuator typically has a very limited travel range, which results in the actuator saturation problem.

A variety of approaches have been reported to deal with the dual-stage control problems. For example, control design for track following and settling can be found in [8]–[10]. The secondary actuator saturation problem is explicitly taken into account during the control design [11], [12]. In [13], a decoupled track-seeking controller using a three-step design approach is developed to enable high-speed one-track seeking and short-span track-seeking for a dual-stage servo system. The control design for the secondary actuator by minimizing the destructive interference is proposed in [14] to attain desired time and frequency responses.

In this brief, we consider a class of DSA systems that can be depicted by Fig. 1(a), where M and m represent the mass of the primary and secondary actuator, respectively. Fig. 1(b) shows an example of our developed DSA positioning system, which consists of a primary stage driven by a linear motor (LM) and a secondary stage driven by a piezo actuator (PA). The secondary actuator has a limited travel range denoted by $\bar{y}_2$, which is very small relative to that of the primary actuator. Under the assumption of $M \gg m$, $|(y_1/y_2)| \gg 1$, and $|(u_2/u_1)| \gg m/M$, we can simply ignore the coupling forces between the two actuators and the dynamic equations of the DSA system are given by

$$\begin{cases} M\ddot{y}_1 = \hat{u}_1 - f - d \\ m\ddot{y}_2 = u_2 - c_0\dot{y}_2 - k_0 y_2 \end{cases} \tag{1}$$

where the friction force f is modeled as the following equation:

$$f = f_c \mathrm{sgn}(\dot{y}_1) + k_v \dot{y}_1 + \Delta \tag{2}$$

where f_c represents the Coulomb friction level, k_v is the viscous friction coefficient and Δ is the unmodeled friction.

By far, most of the work on the DSA tracking control to follow a step command input is based on the strategy that the primary actuator control loop is designed to have little overshoot, and the secondary actuator control loop is designed to follow the position error of the primary actuator [13]–[15]. Under this conventional strategy, the total settling time can be reduced by the time that it takes for the secondary actuator to reach its travel limit. However, when the setpoint is beyond the secondary actuator travel range, this strategy is unable to minimize the total settling time. To further reduce the settling time under this circumstance, we propose that the primary actuator controller can be designed to yield a closed-loop system with a small damping ratio for a fast rise time allowing a certain level of overshoot, and then as the primary actuator approaches the setpoint the secondary actuator control loop is used to reduce the overshoot caused by the primary actuator. In this way, the total settling time is much less than that of the conventional control provided

The authors are with the School of Electrical Engineering and Computer Science, The University of Newcastle, Callaghan, NSW 2308, Australia (e-mail: jinchuan.zheng@newcastle.edu.au; minyue.fu@newcastle.edu.au).
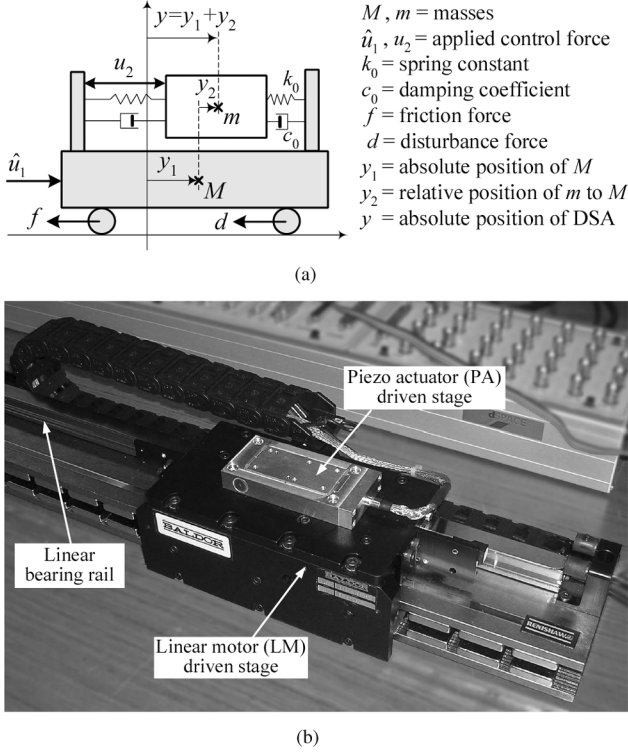
Fig. 1. DSA systems. (a) Illustration of a DSA model. (b) A developed DSA positioning system.

that the overshoot is within the secondary actuator travel range. A similar control strategy for a DSA model without passive coupling between the two stages has been investigated in [16], where the primary actuator overshoots to the amount of the secondary actuator travel range and retains this overshoot in steady state. However, since we consider that the secondary actuator is coupled with the primary actuator through a spring-damper element, our control strategy differs in that the primary actuator overshoots but returns to the target position in steady state, which implies that the secondary actuator has no relative displacement to the primary actuator and as such does not require a constant control input in steady state.

To perform the aforementioned control strategy, Section II presents a nonlinear tracking control method for the DSA systems in Fig. 1(a). We first design a friction compensator followed by a proximate time-optimal controller for the primary actuator to achieve a quick rise time. Then, a composite nonlinear control law for the secondary actuator is developed by a step-by-step procedure. The composite nonlinear feedback law will enable the secondary actuator to reduce the overshoot caused by the primary actuator as the system output approaches the setpoint. Experimental results in Section III show that our proposed control can significantly speed up the responses compared with the conventional control.

II. NONLINEAR FEEDBACK CONTROL DESIGN

Our objective here is to design a control law such that the two actuators cooperate to enable the total position output y to track a step command input of amplitude y_r rapidly with no overshoot larger than 1 μm. In this section, we first present friction compensation for the primary actuator, and then a time-optimal control law is designed to yield a primary closed-loop system
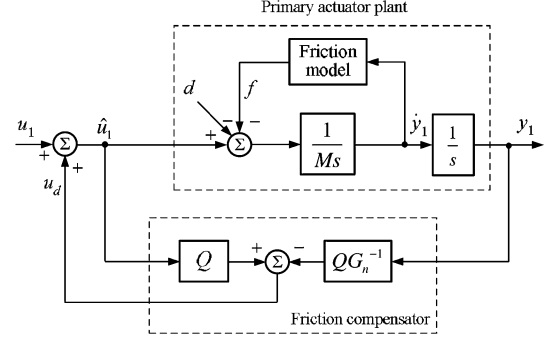

Fig. 2. Block diagram of friction compensation for the primary actuator.

with a small damping ratio so as to achieve a quick rise time. Next, a composite nonlinear control law is designed for the secondary actuator to cause the DSA closed-loop system dynamics to be highly damped as the total position output approaches the setpoint, and thus, the secondary actuator is enabled to reduce the overshoot caused by the primary actuator.

A. Friction Compensation

The nonlinear friction exerts adverse effects on the tracking performance. Here, we employ the model-based control structure as shown in Fig. 2 to compensate for the friction f and disturbance d. The friction compensator is given by

$$G_n = \frac{1}{Ms^2} \tag{3}$$

$$Q = \frac{3\tau s + 1}{(\tau s)^3 + 3(\tau s)^2 + 3\tau s + 1} \tag{4}$$

where τ is a time constant chosen as 5 to 10 times the servo bandwidth such that the filter Q [17] can be approximated as $Q \approx 1$ within the bandwidth of interest. When the friction compensator is applied, the input–output relationship in Fig. 2 can be derived as

$$y_1 = \frac{u_1 - (1 - Q)(d + f)}{Ms^2} \approx \frac{1}{Ms^2}u_1. \tag{5}$$

It can be seen that the nonlinear friction and disturbance are approximately canceled by the friction compensator and the primary actuator system from u_1 to y_1 can be treated as a linear model with a pure double integrator, which facilitates the design of u_1 to further achieve desired performance.

From now on, we take (5) as the model of the primary actuator system and then rewrite the DSA model (1) in a state-space form as follows:

$$\begin{cases} \Sigma_1 : \dot{x}_1 = A_1 x_1 + B_1 u_1, \quad x_1(0) = 0 \\ \Sigma_2 : \dot{x}_2 = A_2 x_2 + B_2 \text{sat}(u_2), \quad x_2(0) = 0 \\ y = y_1 + y_2 = C_1 x_1 + C_2 x_2 \end{cases} \tag{6}$$

where the state $x_1 = [y_1 \ \dot{y}_1]^T, x_2 = [y_2 \ \dot{y}_2]^T$, and

$$A_1 = \begin{bmatrix} 0 & 1 \\ 0 & 0 \end{bmatrix} \quad B_1 = \begin{bmatrix} 0 \\ b_1 \end{bmatrix} \quad C_1 = [1 \quad 0]$$

$$A_2 = \begin{bmatrix} 0 & 1 \\ a_1 & a_2 \end{bmatrix} \quad B_P = \begin{bmatrix} 0 \\ b_2 \end{bmatrix} \quad C_2 = [1 \quad 0]$$

with $b_1 = (1/M), a_1 = -(k_0/m), a_2 = -(c_0/m)$, and $b_2 = (1/m)$. It is clear that A_2 is Hurwitz and the limited travel range

of the secondary actuator is equivalently translated into input constraint with the saturation function $\mathrm{sat}(u_2)$ defined as

$$\mathrm{sat}(u_2) = \mathrm{sgn}(u_2)\min\{\bar{u}_2, |u_2|\} \tag{7}$$

where $\bar{u}_2$ is the saturation level of the control input. Moreover, we assume that the states x_1 and x_2 are all measurable. Hence, the following control law for the DSA system (6) is based on full state feedback.

B. Primary Actuator Control Design

The role of the primary actuator is to provide large travel range beyond that of the secondary actuator. Thus, time optimal control is critical to move the position output quickly from one point to another. The proximate time-optimal servomechanism (PTOS) is a practical near time-optimal controller that can accommodate plant uncertainty and measurement noise. Hence, we apply the PTOS control law [18] to the primary actuator Σ_1 in (6) and the controller is independent of the secondary actuator control loop. The PTOS control law is given by

$$u_1 = \mathrm{sat}[k_2(f(e_1) - \dot{y}_1)] \tag{8}$$

$$f(e_1) = \begin{cases} \frac{k_1}{k_2}e_1, & \text{for } |e_1| \le y_l \\ \mathrm{sgn}(e_1)\left(\sqrt{2\bar{u}_1 b_1 \alpha |e_1|} - \frac{\bar{u}_1}{k_2}\right), & \text{for } |e_1| > y_l \end{cases} \tag{9}$$

$$e_1 = y_r - y_1 \tag{10}$$

where $\mathrm{sat}[\cdot]$ is with the saturation level of $\bar{u}_1$, $\alpha(0 < \alpha < 1)$ is referred to as the acceleration discount factor, k_1 and k_2 are constant gains, and y_l represents the size of a linear region. To make the functions $f(e_1)$ and $f'(e_1)$ continuous such that the control input remains continuous as well, we have the following constraints:

$$\alpha = \frac{2k_1}{b_1 k_2^2} \tag{11}$$

$$y_l = \frac{\bar{u}_1}{k_1}. \tag{12}$$

The PTOS control law introduces a linear region close to the setpoint to reduce the control chatter. In the region $|e_1| \le y_l$, the control is linear and thus the gain $K = [k_1 \ k_2]$ can be designed by any linear control techniques. For instance, using the pole-placement method [19], we obtain a parameterized state feedback gain K as follows:

$$K = \frac{1}{b_1}\left[4\pi^2\omega_1^2 \ 4\pi\omega_1\zeta_1\right] \tag{13}$$

where ζ_1 and ω_1 (hertz), respectively, represent the damping ratio and undamped natural frequency of the closed-loop system $C_1(sI - A_1 + B_1 K)^{-1}B_1$, whose poles are placed at $2\pi\omega_1(-\zeta_1 \pm j\sqrt{1 - \zeta_1^2})$.

In conventional DSA control systems, the primary actuator controller is generally designed to have little overshoot such as by choosing a large damping ratio in (13). However, in our proposed control a small damping ratio is chosen for a fast rise time and the resultant overshoot is within the secondary actuator travel limit, which can be then reduced by the secondary actu-

ator under a composite nonlinear control law as will be given in the next subsection. Thus, the settling time in the proposed control could be less than that in the conventional control.

C. Secondary Actuator Control Design

The goal of the control design for the secondary actuator Σ_2 in (6) is to enable the secondary actuator to reduce the overshoot caused by the primary actuator. We have the following step-by-step design procedure.

Step 1) Design a linear feedback control law

$$u_{2L} = Fx_2 \tag{14}$$

where $F = [f_1 \ f_2]$ is chosen such that the secondary actuator control system as given by

$$\dot{x}_2 = A_2 x_2 + B_2 \mathrm{sat}(Fx_2) \tag{15}$$

is globally asymptotically stable (GAS) and the corresponding closed-loop system in the absence of input saturation, $C_2(sI - A_2 - B_2F)^{-1}B_2$, has a larger damping ratio and a higher undamped natural frequency than those of the primary actuator control loop. To do this, we choose

$$F = -B_2^T P \tag{16}$$

where $P = P^T > 0$ is the solution of the following Lyapunov equation:

$$A_2^T P + PA_2 = -Q \tag{17}$$

for a given $Q = Q^T > 0$. Note that the solution of P exists since A_2 is Hurwitz. To involve the closed-loop properties explicitly with the control law, we define

$$Q = \begin{bmatrix} q_1 & 0 \\ 0 & q_2 \end{bmatrix} \quad q_1 > 0 \quad q_2 > 0 \tag{18}$$

where q_1 and q_2 are tuning parameters. Substituting (18) into (17) yields P, which gives the feedback gain (16) as follows:

$$F = \frac{b_2}{2a_1 a_2}[a_2 q_1 \ a_1 q_2 - q_1]. \tag{19}$$

Moreover, the resulting poles of the closed-loop system $C_2(sI - A_2 - B_2F)^{-1}B_2$ with (19) if complex conjugate have the undamped natural frequency and damping ratio as follows:

$$\omega_2 = \frac{1}{2\pi}\sqrt{-\frac{b_2^2}{2a_1}q_1 - a_1}$$

$$\zeta_2 = \frac{b_2^2 q_1 - b_2^2 a_1 q_2 - 2a_1 a_2^2}{4a_1 a_2 \sqrt{-\frac{b_2^2}{2a_1}q_1 - a_1}}.$$

Thus, we can easily achieve the desired ω_2 and ζ_2 by choosing a proper pair of q_1 and q_2.

Step 2) Construct the nonlinear feedback control law

$$u_{2N} = \gamma(y_r, y) H \begin{bmatrix} y_1 - y_r \\ \dot{y}_1 \end{bmatrix} \qquad (20)$$

$$H = \frac{1}{b_2}[(a_1 + b_2 f_1 + b_1 k_1) \quad (a_2 + b_2 f_2 + b_1 k_2)] \quad (21)$$

where H is taken to achieve desired closed-loop system dynamics, which will be clear later; and $\gamma(y_r, y)$ is any nonnegative function locally Lipschitz in y, which is chosen to enable the secondary actuator to reduce the overshoot caused by the primary actuator as the total position output approaches the setpoint. The choice of $\gamma(y_r, y)$ will be discussed later.

Step 3) Combine the linear and nonlinear feedback control laws derived in Steps 2) and 3) to form a composite nonlinear controller for the secondary actuator

$$u_2 = u_{1L} + u_{2N} = Fx_2 + \gamma(y_r, y) H \begin{bmatrix} y_1 - y_r \\ \dot{y}_1 \end{bmatrix}. \quad (22)$$

With the primary actuator controller in (8) and the secondary actuator controller as given by (22), we have the following results regarding the step response of the DSA closed-loop system.

Lemma 1: Consider the DSA system in (6) with the primary actuator Σ_1 under the PTOS control law (8) and the secondary actuator Σ_2 under the nonlinear control law (22) for any nonnegative function $\gamma(y_r, y)$ locally Lipschitz in y. Then, the composite control law will drive the total system output y to track asymptotically any step command input of amplitude y_r.

Proof: The primary actuator closed-loop system under the PTOS control law can be represented as

$$\dot{x}_1 = A_1 x_1 + B_1 \text{sat}[k_2(f(e_1) - \dot{y}_1)] \quad (23)$$

where $f(e_1)$ is defined in (9). It has been proven in [18] that the system (23) can track asymptotically any step command input of amplitude y_r, i.e.,

$$\lim_{t \to \infty} y_1(t) = y_r \qquad \lim_{t \to \infty} \dot{y}_1(t) = 0. \quad (24)$$

Next, we define a Lyapunov function $V = x_2^T P x_2$ with P given in (17). Evaluating the derivative of V along the trajectories of the system in (15) yields

$$\begin{aligned}
\dot{V} &= \dot{x}_2^T P x_2 + x_2^T P \dot{x}_2 \\
&= x_2^T \left(A_2^T P + P A_2 \right) x_2 + 2 B_2^T P x_2 \text{sat}(Fx_2) \\
&= -x_2^T Q x_2 - 2 F x_2 \text{sat}(Fx_2) \\
&\leq -x_2^T Q x_2 \\
&< 0.
\end{aligned} \quad (25)$$

Hence, the secondary actuator closed-loop system with linear feedback control only (15) is GAS. Furthermore, the secondary actuator closed-loop system with the composite nonlinear control law (22) can be expressed as

$$\dot{x}_2 = A_2 x_2 + B_2 \text{sat}(Fx_2 + u_{2N}). \quad (26)$$

It is obvious that the system (26) satisfies the converging-input bounded-state (CIBS) property (see the Appendix for the definition) since A_2 is Hurwitz, $|\text{sat}(\cdot)| \leq \bar{u}_2$, and the nonlinear control input u_{2N} has

$$\lim_{t \to \infty} u_{2N}(t) = 0 \quad (27)$$

which can be easily deduced from (20) and (24).

The proof finishes by observing that the DSA closed-loop system formed by (23) and (26) has a cascaded structure and it satisfies the conditions of Theorem 1 in the Appendix. This result will guarantee that the secondary actuator closed-loop system (26) is GAS at the origin. Thus, for any initial state $x_2(0)$ and nonlinear control input that satisfies (27) we have

$$\lim_{t \to \infty} x_2(t) = 0 \quad (28)$$

and, therefore

$$\lim_{t \to \infty} y(t) = \lim_{t \to \infty} [C_1 x_1(t) + C_2 x_2(t)] = y_r. \quad (29)$$

Remark 1: Lemma 1 shows that the value of $\gamma(y_r, y)$ does not affect the ability of the overall DSA closed-loop system to track asymptotically any step command input. However, a proper choice of $\gamma(y_r, y)$ can be utilized to improve the transient performance of the overall closed-loop system. This is the key property of the proposed control design.

D. Selecting $\gamma(y_r, y)$ for Improved Performance

The function $\gamma(y_r, y)$ is used to tune the control law to achieve our objective. More specifically, we design the primary actuator control loop with a small damping ratio for a quick rise time and employ the secondary actuator control loop that is designed to be highly damped to reduce the overshoot caused by the primary actuator as the total position output y approaches the setpoint. This control strategy implies that the dynamics of the DSA closed-loop system should be dominated by the primary actuator control loop when the position output is far away from the setpoint, but dominated by the secondary actuator control loop when the position output approaches the setpoint. The purpose of the function $\gamma(y_r, y)$ is to provide a smooth transition from the primary control loop to the secondary control loop.

Consider the dual-stage system (6) with the control laws in (8) and (22), and assume that the tracking error $(y_r - y)$ is small such that the control inputs do not exceed the limits and the control law (8) works within its linear region. Thus, the DSA closed-loop system can be expressed as

$$\Sigma : \begin{cases} \dot{x} = Ax + By_r \\ y = Cx \end{cases} \quad (30)$$

where

$$A = \begin{bmatrix} A_1 - B_1 K & 0 \\ \gamma(y_r, y) B_2 H & A_2 + B_2 F \end{bmatrix}$$

$$B = \begin{bmatrix} B_1 K \\ -\gamma(y_r, y) B_2 H \end{bmatrix} \cdot \begin{bmatrix} 1 \\ 0 \end{bmatrix}$$

$$C = [C_1 \ C_2].$$

Since the nonlinear term $\gamma(y_r, y)$ makes the system dynamics difficult to analyze, we assume that $\gamma(y_r, y)$ varies slowly with respect to y and thus we can reasonably approximate $\gamma(y_r, y)$ as a constant in a local region for easy analysis of the DSA system dynamics. Thus, the DSA closed-loop system dynamics can be represented by the following transfer function from y_r to y:

$$G(s) = C(sI - A)^{-1}B = (1 - \gamma)G_1(s) + \gamma G_2(s) \quad (31)$$

where

$$G_1(s) = \frac{b_1 k_1}{s^2 + b_1 k_2 s + b_1 k_1} \quad (32)$$

$$G_2(s) = \frac{-(a_1 + b_2 f_1)}{s^2 - (a_2 + b_2 f_2)s - (a_1 + b_2 f_1)} \quad (33)$$

indicate the closed-loop transfer function of the primary and secondary actuator control loop, respectively.

In (31), when γ monotonically increases from 0 to 1, it is clear that $G(s)$ changes from $G_1(s)$ to $G_2(s)$. This desired feature is due to the proper selection of H in (21). From the perspective of zero placement, when γ changes from 0 to 1 the zeros of (31) are moved from the pole locations of the secondary control loop (32) to those of the primary control loop (33). Since the zeros near the poles reduce the effects of the poles on the total response, we can use γ to tune the system dynamics for desired performance. A similar control technique for single-input–single-output (SISO) linear systems can be found in [20], which however uses the nonlinear feedback law to increase the damping ratio of the closed-loop system poles to reduce the overshoot.

Based on the preceding analysis, we may choose γ as a function of the tracking error (i.e., $y_r - y$) such that $\gamma(y_r, y)$ monotonically increases from 0 to 1 as $y \to y_r$. The following shows one choice of γ:

$$\gamma(y_r, y) = e^{-\beta|y_r - y|} \quad (34)$$

where $\beta \geq 0$ is a tuning parameter, which can be adjusted with respect to the amplitude of y_r relative to the secondary actuator travel limit $\bar{y}_2$.

1) If $y_r \leq \bar{y}_2$, β should be sufficiently small such that γ converges to 1 quickly, which implies that the secondary control loop dominates the DSA closed-loop system dynamics over the whole control stage. In this case, the total settling time can be minimized because the secondary control loop has a much faster bandwidth than that of the primary control loop.

2) If $y_r > \bar{y}_2$, β should be large so as to divide the control stages into two parts. At the initial stage when the position output y is far away from the final setpoint, γ closes to 0, which implies that the primary control loop dominates the DSA closed-loop system dynamics to achieve a fast rise time while the secondary actuator is switched off because of its limited travel range. When the position output y approaches the setpoint, γ is close to 1, which implies that the DSA closed-loop system dynamics is dominated by the secondary control loop that is highly damped. This high
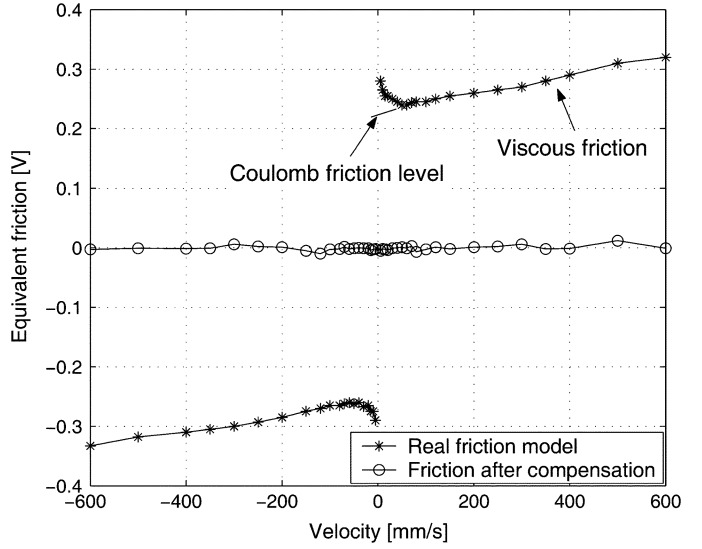

Fig. 3. Experimental friction model of the LM driven stage. (The vertical axis denotes the steady-state control input u_1 in Fig. 2 that compensates for the friction force to make the LM move at the corresponding constant velocity.)

damping property can in turn imply that the secondary actuator is enabled to reduce the overshoot caused by the primary actuator.

III. EXPERIMENTAL RESULTS

This section presents the experimental results of the proposed nonlinear control method applied to the actual DSA positioning system as shown in Fig. 1(b).

A. System Modeling

The LM in Fig. 1(b) has a 0.5-m travel range, a 1-μm resolution glass scale encoder, and a power amplifier. The PA has a maximum travel range of ± 15 μm, a piezoelectric amplifier, and an integrated capacitive position feedback sensor with 0.2-nm resolution to measure the relative displacement between the PA stage and the LM stage. The resonance of the PA stage flexure is actively damped by its integrated control electronics. Moreover, we observe that the coupling effects between the two actuator stages on the position output is much less than 1 μm. Hence, we assume that there is no coupling between the LM and PA system.

The nonlinear friction model in the LM is measured using the experimental method in [21] and shown in Fig. 3. The friction compensator in Fig. 2 is obtained by using $\tau = 0.0008$ and $M = 6.7 \times 10^{-8}$. It can be seen from Fig. 3 that the nonlinear friction is almost compensated by the friction compensator. Thus, the DSA positioning system can be expressed by (6), the parameters of which are then identified from experimental frequency response data. A dynamic signal analyzer (HP 35670A, Hewlett Packard Company, WA) is used to generate the swept-sinusoidal excitation signals and collect the frequency response data from the excitation signals to the output. The dashed lines in Figs. 4 and 5 show the measured frequency responses of the LM and PA stage. The LM dynamics are dominated by the rigid body mode and thus close to a double integrator. The PA dynamics is of high stiffness that exhibits a flat gain in the low
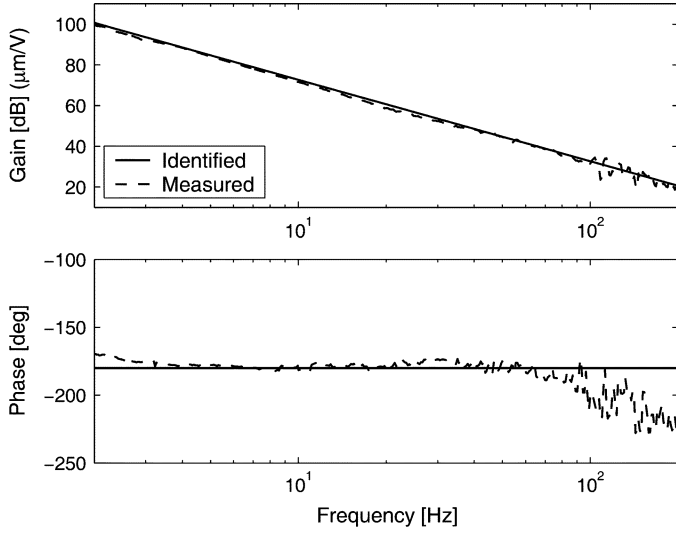
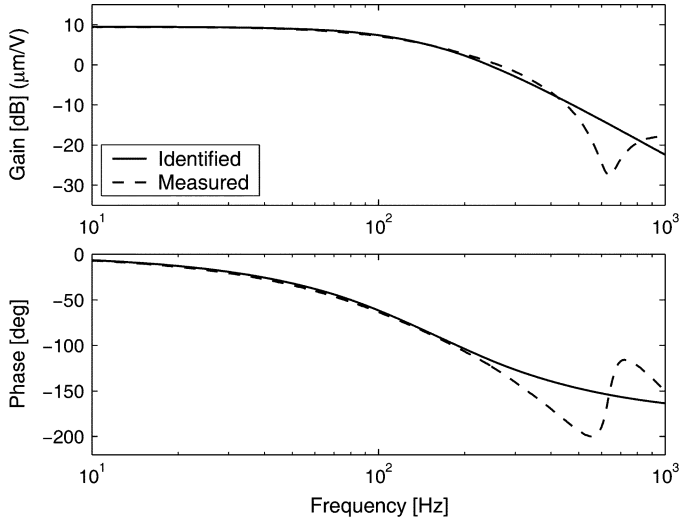Fig. 4.   Frequency responses of the LM model from u_1 to y_1 in Fig. 2 with the friction compensator.

Fig. 5.   Frequency responses of the PA stage, the PA gain is 3 μm/V.

frequency range. By using the least-squares estimation method [22], we obtain the DSA model parameters in (6) as follows:

$$b_1 = 1.5 \times 10^7 \quad a_1 = -10^6 \quad a_2 = -1810 \tag{35}$$

$$b_2 = 3 \times 10^6 \quad \bar{u}_2 = 5 \text{ V}. \tag{36}$$

The solid lines in Figs. 4 and 5 show that the identified models match the measured models well in the frequency range of interest.
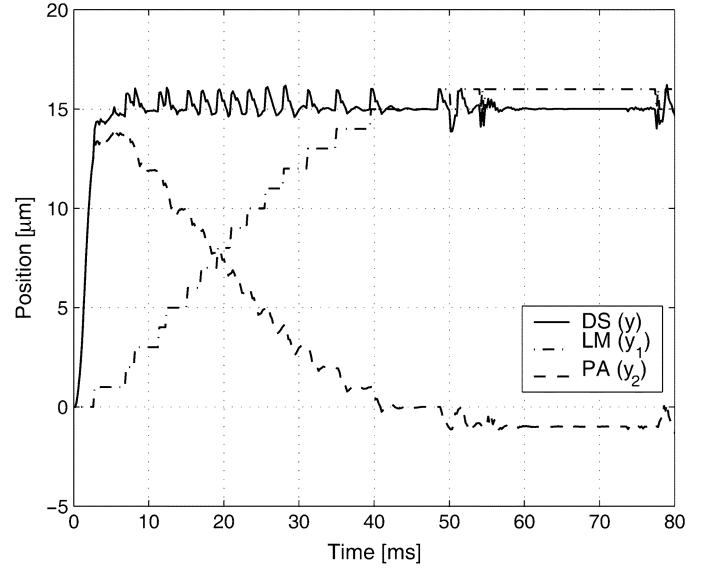
B. Results and Discussion

We follow the proposed control design procedure to obtain the controller for the DSA positioning system. The PTOS controller in (8) for the LM is obtained by choosing $\bar{u}_1 = 1$ V, $\omega_1 = 30$ Hz, and thus $y_l = 422 \mu$m. We find that ζ_1 can be adjusted as

$$\zeta_1(y_r) = \begin{cases} 0.5, & y_r \le 15 \,\mu\text{m} \\ \dfrac{2.7 - \ln(y_r)}{\sqrt{\pi^2 + [2.7 - \ln(y_r)]^2}}, & y_r > 15 \,\mu\text{m} \end{cases} \tag{37}$$
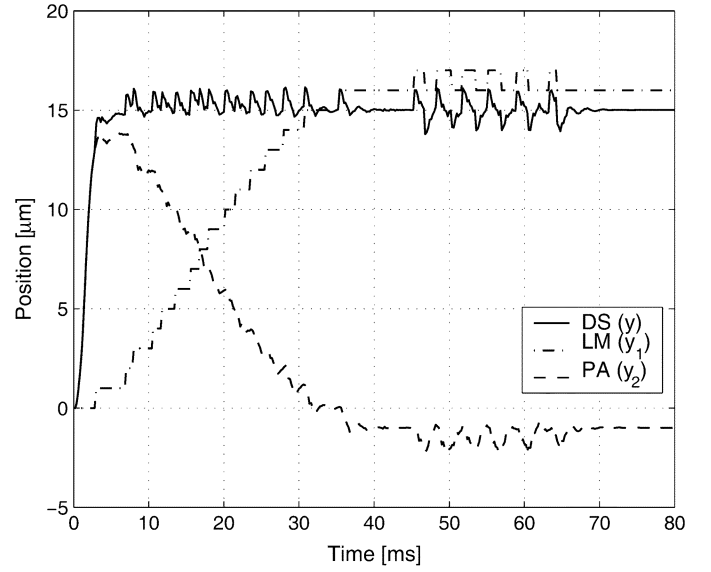
(a)

(b)

Fig. 6.   Dual-stage tracking control for $y_r = 15 \,\mu$m. The settling times in both control are similarly 4 ms. The proposed control has little improvement over the conventional control because within the PA travel limit the PA control loop dominates the DSA closed-loop system dynamics whatever the LM control loop is tuned. (a) Proposed control. (b) Conventional control.

such that the resultant overshoot caused by the LM approximately equals to the PA travel limit, i.e., 15 μm, when $y_r > 15 \,\mu$m. Hence, the linear gain K is given by
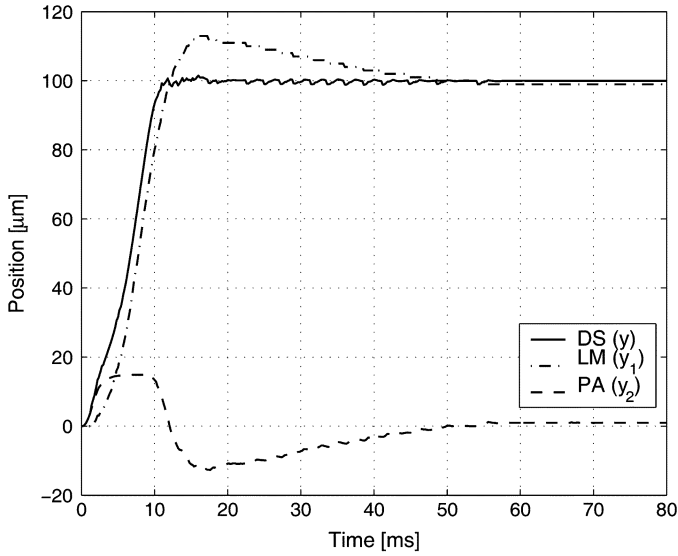
$$K = 10^{-3} \times [2.4 \quad 0.025\zeta_1(y_r)]. \tag{38}$$

For the PA control design, we choose $q_1 = 0.56$ and $q_2 = 7 \times 10^{-8}$, and thus the linear feedback gain F is given by
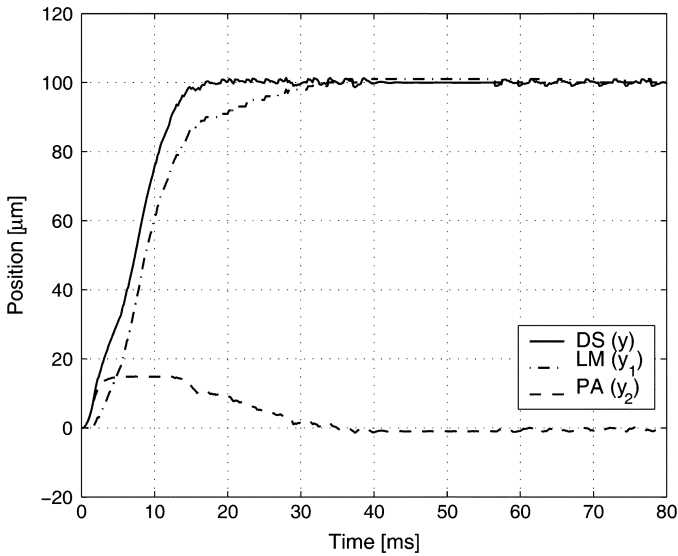
$$F = -[0.8385 \quad 0.0005] \tag{39}$$

which results in $\omega_2 = 300$ Hz and $\zeta_2 = 0.9$. The nonlinear feedback gain is given by

$$H = -[1.1602 \quad 0.0011 - 0.00012\zeta_1(y_r)] \tag{40}$$
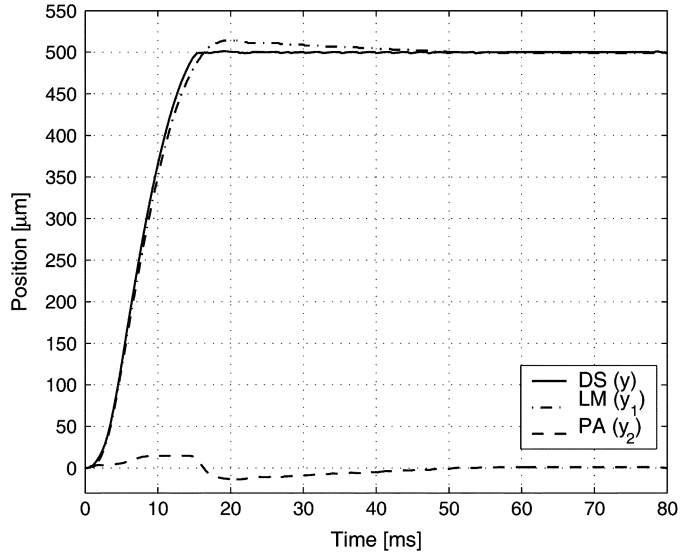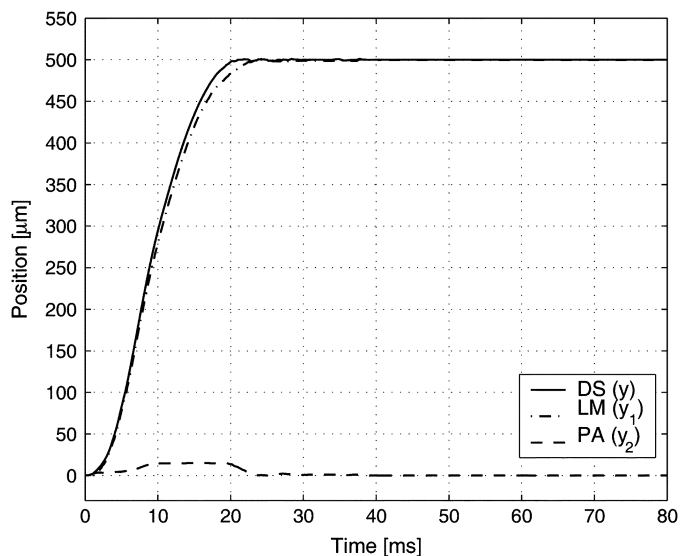
Fig. 7. Dual-stage tracking control for $y_r = 100\ \mu$m. The settling time in the conventional control is 16.5 ms, which is reduced to 11 ms in the proposed control. (a) Proposed control. (b) Conventional control.

Fig. 8. Dual-stage tracking control for $y_r = 500\ \mu$m. The settling time in the conventional control is 20 ms, which is reduced to 15.5 ms in the proposed control. (a) Proposed control. (b) Conventional control.

with $\zeta_1(y_r)$ in (37). The nonlinear function (34) is chosen as

$$\gamma(y_r, y) = \begin{cases} e^{-0.001|y-y_r|}, & y_r \leq 15\ \mu\text{m} \\ e^{-0.01|y-y_r|}, & y_r > 15\ \mu\text{m}. \end{cases} \quad (41)$$

In order to compare the proposed control with the conventional control where the LM control loop is generally tuned to have no overshoot, we choose $\zeta_1 = 0.9$ for any y_r and retain the other tuning parameters, then following the same design procedure yields a conventional controller that is used for comparison with our proposed controller. Moreover, we define the settling time to be the time that it takes for the total position output y to enter and remain within $\pm 1\ \mu$m relative to the setpoint.

The controllers are implemented by a real-time DSP system (dSPACE-DS1103) with the sampling frequency of 5 kHz. The velocities of the LM and PA stage are estimated using backward differentiating their position signals, respectively. The experimental results for various travel distance ($y_r = 15, 100, 500\ \mu$m) are shown in Figs. 6–8, respectively. In Fig. 6, where the travel distance is within the PA travel range, the settling times under the proposed control and the conventional control are almost the same. However, when the travel distance is beyond the PA travel range as shown in Figs. 7 and 8, the settling time under the proposed control is significantly reduced compared with the conventional control. The experiments with 50, 300, and 1000 μm travel distance are also implemented. All the implementation results in terms of settling time are summarized in Table I for easy comparison. It is shown that the proposed control can further reduce the settling time by more than 20% when the travel distances are beyond 15 μm.

TABLE I
COMPARISON OF THE SETTLING TIME IMPROVEMENT

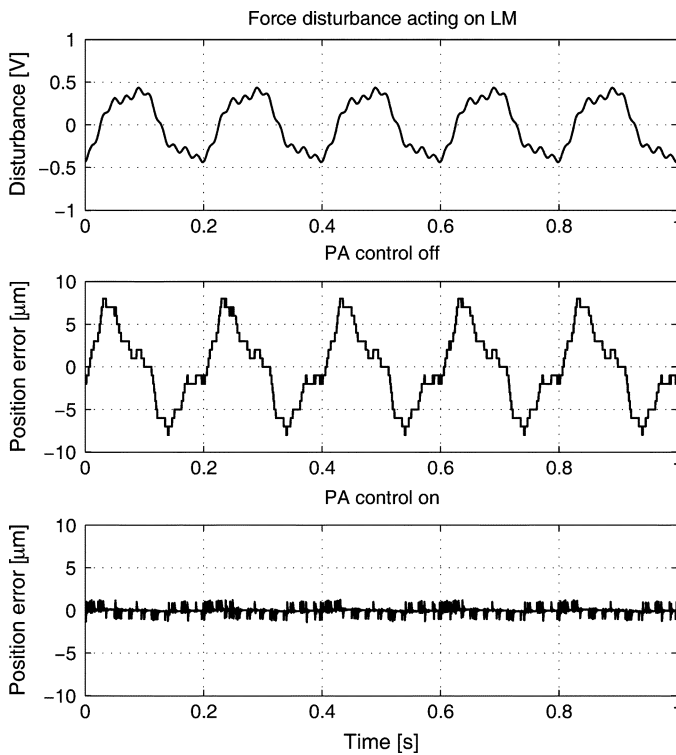| Travel distance (μm)	Settling Time (ms)		Improvement (%)
	Conventional	Proposed	
15	4	4	0
50	12.5	10	20
100	16.5	11	33
300	20	14	30
500	21	15.5	26
1000	26	20	23

Fig. 9. Steady-state position error under disturbance input. When PA control is switched off, the position error under the LM control loop is within $\pm 8\,\mu$m, while with PA control on, the position error is retained within $\pm 1\,\mu$m.

Finally, we test the performance of the proposed dual-stage control system under disturbance input. The disturbance signal as shown in the top plot of Fig. 9 consists of three sinusoidal components with frequencies at 5, 15, and 50 Hz. The signals are artificially generated in DSP and directly added onto the LM control input, which can be reasonably assumed as force disturbance acting on the LM stage. In Fig. 9, the middle plot shows that the LM control loop can only maintain the steady-state position error within $\pm 8\,\mu$m, while the bottom plot shows that the position error is reduced to within $\pm 1\,\mu$m when the PA control loop is switched on. Thus, the results indicate that the proposed control can achieve improved positioning accuracy over the single-stage control.

IV. CONCLUSION

In this brief, we have proposed a nonlinear control method for DSA systems. Distinct from the conventional control, the primary actuator control loop is designed to have a small damping ratio for a fast rise time. The secondary actuator control loop is then enabled by a nonlinear control law to reduce the overshoot caused by the primary actuator as the system output approaches the setpoint. We have also verified the proposed control on an actual DSA positioning system. Experimental results demonstrate that it can further reduce the settling time by more than 20% compared with the conventional control. Moreover, it is shown that the DSA positioning system with the proposed control can achieve more accurate position accuracy under external disturbance than that of the single-stage servo with LM only. Our future work will extend the nonlinear control design to higher order systems and the case of output feedback.

APPENDIX

Consider a cascade system as follows:

$$\dot{x} = f(x,y) \quad f(0,0) = 0 \tag{42}$$
$$\dot{y} = g(y) \quad g(0) = 0 \tag{43}$$

where f and g are smooth, x and y evolve in $\mathbb{R}^n$ and $\mathbb{R}^m$, respectively. Define the zero-input system of (42) as

$$\dot{x} = f(x,0) \tag{44}$$

and the converging input bounded state (CIBS) property as follows.

CIBS: For each control $y(\cdot)$ on $[0,+\infty)$ such that $\lim_{t\to\infty} y(t) = 0$ and for each initial state x_0, the solution of (42) with $x(0) = x_0$ exists for all $t \geq 0$ and is bounded.

Theorem 1 [23]: Assume that both (43) and (44) have the origin as a globally asymptotically stable state and the CIBS property holds for (42). Then the cascade system of (42) and (43) has the origin as a globally asymptotically stable state.

REFERENCES

[1] K. Mori, T. Munemoto, H. Otsuki, Y. Yamaguchi, and K. Akagi, "A dual-stage magnetic disk drive actuator using a piezoelectric device for a high track density," *IEEE Trans. Magn.*, vol. 27, no. 6, pp. 5298–5300, Nov. 1991.
[2] R. Evans, J. Griesbach, and W. Messner, "Piezoelectric microactuator for dual stage control," *IEEE Trans. Magn.*, vol. 35, no. 2, pp. 977–982, Mar. 1999.
[3] L. Guo, D. Martin, and D. Brunnett, "Dual-stage actuator servo control for high density disk drives," in *Proc. IEEE/ASME Int. Conf. Adv. Intel. Mechatron.*, 1999, pp. 132–137.
[4] B. Kim, J. Li, and T. Tsao, "Two-parameter robust repetitive control with application to a novel dual-stage actuator for noncircular machining," *IEEE/ASME Trans. Mechatron.*, vol. 9, no. 4, pp. 644–652, Dec. 2004.

[5] S. Kwon, W. Chung, and Y. Youm, "On the coarse/fine dual-stage manipulators with robust perturbation compensator," in *Proc. IEEE Int. Conf. Robot. Autom.*, 2001, pp. 121–126.

[6] A. Elfizy, G. Bone, and M. Elbestawi, "Design and control of a dual-stage feed drive," *Int. J. Machine Tools Manuf.*, vol. 45, pp. 153–165, 2005.

[7] W. Yao and M. Tomizuka, "Robust controller design for a dual-stage positioning system," in *Proc. Int. Conf. Ind. Electron., Control, Instrum.*, 1993, pp. 62–66.

[8] S. Schroeck, W. Messner, and R. McNab, "On compensator design for linear time-invariant dual-input single-output systems," *IEEE/ASME Trans. Mechatron.*, vol. 6, no. 1, pp. 50–57, Mar. 2001.

[9] X. Huang and R. Horowitz, "Robust controller design of a dual-stage disk drive servo system with an instrumented suspension," *IEEE Trans. Magn.*, vol. 41, no. 8, pp. 2406–2413, Aug. 2005.

[10] H. Numasato and M. Tomizuka, "Settling control and performance of a dual-actuator system for hard disk drives," *IEEE/ASME Trans. Mechatron.*, vol. 8, no. 4, pp. 431–438, Dec. 2003.

[11] G. Herrmann, M. Turner, I. Postlethwaite, and G. Guo, "Practical implementation of a novel anti-windup scheme in a HDD-dual-stage servo system," *IEEE/ASME Trans. Mechatron.*, vol. 9, no. 3, pp. 580–592, Sep. 2004.

[12] T. Shen and M. Fu, "High precision and feedback control design for dual-actuator systems," in *Proc. IEEE Conf. Control Appl.*, 2005, pp. 956–961.

[13] M. Kobayashi and R. Horowitz, "Track seek control for hard disk dual-stage servo systems," *IEEE Trans. Magn.*, vol. 37, no. 2, pp. 949–954, Mar. 2001.

[14] S. Lee and Y. Kim, "Minimum destructive interference design of dual-stage control systems for hard disk drives," *IEEE Trans. Control Syst. Technol.*, vol. 12, no. 4, pp. 517–531, Jul. 2004.

[15] B. Hredzak, G. Herrmann, and G. Guo, "A proximate-time-optimal control design and its application to a hard disk drive dual-stage actuator system," *IEEE Trans. Magn.*, vol. 42, no. 6, pp. 1708–1715, Jun. 2006.

[16] J. McCormick and R. Horowitz, "Time optimal seek trajectories for a dual-stage optical disk drive actuator," *J. Dyn. Syst., Meas., Control*, vol. 113, pp. 534–536, Sep. 1991.

[17] H. Choi, B. Kim, I. Suh, and W. Chung, "Design and robust high-speed motion controller for a plant with actuator saturation," *J. Dyn. Syst., Meas., Control*, vol. 122, pp. 535–541, Sep. 2000.

[18] M. Workman, "Adaptive proximate time-optimal servomechanisms," Ph.D. dissertation, Stanford Univ., Stanford, CA, 1987.

[19] G. F. Franklin, J. D. Powell, and A. Emami-Naeini, *Feedback Control of Dynamic Systems*, 3rd ed.   Reading, MA: Addison-Wesley, 1994.

[20] Z. Lin, M. Pachter, and S. Banda, "Toward improvement of tracking performance—Nonlinear feedback for linear systems," *Int. J. Control*, vol. 70, pp. 1–11, 1998.

[21] E. Papadopoulos and G. Chasparis, "Analysis and model-based control of servomechanisms with friction," in *Proc. IEEE/RSJ Int. Conf. Intell. Robots Syst.*, 2002, pp. 2109–2114.

[22] L. Ljung, *System Identification—Theory for the User*, 2rd ed.   Englewood Cliffs, NJ: Prentice-Hall, 1999.

[23] E. Sontag, "Remarks on stabilization and input-to-state stability," in *Proc. IEEE Conf. Dec. Control*, 1989, pp. 1376–1378.